Parametric amplification in an electromagnetically-induced-transparency medium

Ken-ichi Harada
Japan Science and Technology Agency, 4-1-8 Honmachi, Kawaguchi, 331-0012, Japan

Kenji Mori, Junji Okuma, Nobuhito Hayashi, and Masaharu Mitsunaga*
Graduate School of Science and Technology, Kumamoto University, 2-39-1 Kurokami, Kumamoto, 860-8555, Japan
(Received 5 February 2008; published 8 July 2008)

In an ordinary electromagnetically-induced-transparency (EIT) experiment using a hot sodium vapor, we have observed a probe gain up to 32 in the presence of a coupling beam in an otherwise totally opaque (transmissivity $\sim 10^{-5}$) situation, increasing the transmissivity by 6 orders of magnitude. This gain is attributable to parametric amplification (PA), accompanying the Stokes (or anti-Stokes) wave with similar output intensity, and is critically dependent upon the atomic density and the coupling beam power. Experimental and theoretical analyses have revealed that, while the EIT picture is valid for relatively low atomic densities, the PA picture becomes dominant for high atomic densities and high coupling powers. We have also found that the parametric coupling between the probe and Stokes waves can be nullified by the proper choice of the coupling detuning frequency, due to destructive interference of two elementary processes.

DOI: 10.1103/PhysRevA.78.013809 PACS number(s): 42.65.Dr, 42.50.Gy

I. INTRODUCTION

In recent developments of modern quantum optics, electromagnetically induced transparency (EIT) [1,2] plays one of the most important roles, and its applications range broadly from precision spectroscopy including atomic clocks and magnetometers [3,4], to quantum information science such as light storage and quantum memory [5–8]. In an EIT experiment, as the word "transparency" indicates, the transmissivity T of a probe beam increases in the presence of a strong coupling beam that couples the common excited state to a third level and eventually T becomes close to 1 for higher coupling powers, but T never exceeds 1. This statement may be validated in the original expression (1a) of Ref. 1 for the probe absorption cross section, which is positive for any arbitrary coupling intensity, regardless of whether the medium is homogeneously or inhomogeneously broadened. In terms of the dressed atom theory, strongly dressed excited state by the coupling beam will be Rabi split into two and, in the middle of the spectrum, the probe absorption is greatly reduced. The perfect transparency is obtained when the sublevel coherence decay rate is zero, and in this case the destructive interference is complete. The only way to obtain a probe gain in the framework of EIT would be to further modify the excited-state or the ground-state population by incoherent optical pumping, thus converting the system from a transparent to an amplifying medium, the effect well known as gain without inversion (GWI) or laser without inversion (LWI) [9–11].

The reason why one obtains $T \leq 1$ in a conventional EIT theory stems from the fact that one limits the treatment in the two-mode case, including probe and coupling, whose frequencies ω_p and ω_c are apart from each other by the ground-state hyperfine splitting ω_{21} of the Λ-type three-level system. On the other hand, it has been repeatedly claimed by us [12–15] and by other workers [16,17] that, in EIT experiments, generation of the Stokes wave ($\omega_s = 2\omega_c - \omega_p$) by stimulated Raman scattering (SRS), as the opposite sideband of probe with respect to coupling, is never negligible and is even critically important, and thus the problem must be treated as the three-mode system for ω_p, ω_c, and ω_s. (Throughout this paper we assume $\omega_p > \omega_c$, and a Stokes wave $\omega_s = \omega_c - \omega_{21}$ is generated when $\omega_p - \omega_c = \omega_{21}$. Of course, when $\omega_p < \omega_c$, an anti-Stokes wave $\omega_{as} = \omega_c + \omega_{21}$ can be generated when $\omega_c - \omega_p = \omega_{21}$, but the treatment is the same.)

In this paper, we will experimentally and theoretically show that, even in an ordinary EIT experiment, the probe beam can be amplified in a very dramatic fashion simply by the proper choice of parameters. Experimentally, we have found, by using a hot sodium vapor, that an otherwise extremely opaque medium of $T \sim 10^{-5}$ can become a gain medium of $T \sim 10$ by the presence of coupling beam. This improvement of the output intensity by six orders of magnitudes is accompanied by the generation of the Stokes wave with similar output intensity, thus enabling the whole system described by parametric amplification (PA), where probe and Stokes play the roles of signal and idler. The criterion of whether the system is EIT-like or PA-like is determined by the atomic density N. We will show in this paper that although the EIT picture is valid and $T < 1$ for low N, for high N SRS process is comparable with EIT. Furthermore, as we increase the coupling power in the high N region, the probe and Stokes waves build up simultaneously, grow exponentially and PA prevails. In this region probe transmission T as well as the Stokes gain (defined as the output Stokes intensity divided by the input probe intensity) can easily exceed 1.

Similar types of parametric gain have been reported in rubidium vapor [18,19], but in a transparent frequency region, where the EIT concept does not apply. Also, similar types of gain (Raman gain) and oscillation were observed more than two decades ago by Kumar *et al.* but without any description of parametric processes [20,21], nor the concept

*mitunaga@sci.kumamoto-u.ac.jp

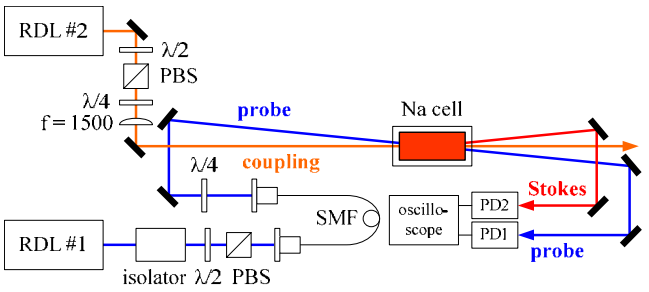

FIG. 1. (Color online) Schematic of the experimental setup. RDL: ring dye laser; PBS: polarizing beam splitter; SMF: single-mode fiber; PD: photodetector.

of EIT. Here in this paper we will treat EIT and PA in a comprehensive manner and nail down the issue of EIT vs PA classification. In the following sections we will first show our experimental results, which are then followed by the theoretical treatment.

II. EXPERIMENT

The experiment was performed in an ordinary EIT setup using two independently tunable single-frequency ring dye lasers (RDL1 and RDL2) tuned to the $3S_{1/2}-3P_{1/2}$ D_1 transition of the Na atom at 589.6 nm. As schematically illustrated in Fig. 1, the two beams (probe and coupling from RDL1 and RDL2, respectively) with the same σ_+ polarizations impinged noncollinearlly (with an angle 4.5 mrad) on the sample of a hot sodium atomic vapor with no buffer gas in a glass cylindrical cell (4.5-cm long) with magnetic shielding. A typical atomic density was 4×10^{11} cm^{-3} corresponding to transmissivity $T\sim10^{-5}$ and typical probe and coupling powers were 1 and 250 mW, respectively. In order to improve the beam quality, a single-mode fiber was employed for the probe beam. Three different types of output beam profiles were observed, as shown in Fig. 2, as the probe frequency ν_p was scanned while the coupling frequency ν_c was fixed at the D_1 resonance. When ν_p was out of the D_1 resonance, the transmitted coupling spot (due to saturated absorption) and the transmitted probe spot (due to off resonance) were seen [Fig. 2(a)]. (The coupling transmissivity was about 50%.) When ν_p was on the D_1 resonance, the probe spot was totally absorbed [Fig. 2(b)] and only the coupling spot was seen. However, when ν_p satisfied the two-photon resonance condition $\nu_p-\nu_c=\pm\nu_{21}$, where $\nu_{21}=1.772$ GHz is the Na hyperfine splitting frequency, the amplified probe spot was observed. In addition to the probe spot, a new spot with similar intensity was observed on the opposite side of the probe, corresponding to the Stokes (anti-Stokes) spot [Fig. 2(c)]. Separate optical frequency measurements using an optical spectrum analyzer showed that the frequency of the new spot was indeed Stokes or anti-Stokes shifted depending on whether $\nu_p-\nu_c=\nu_{21}$ or $-\nu_{21}$. Therefore the Stokes wave satisfied both the energy conservation $\nu_s=2\nu_c-\nu_p$ and the momentum conservation $\vec{k}_s=2\vec{k}_c-\vec{k}_p$.

A typical probe transmission spectrum, measured by PD1, is given in Fig. 3(a) along with a typical intensity spectrum of the Stokes spot, measured by PD2, in Fig. 3(b). In Fig.

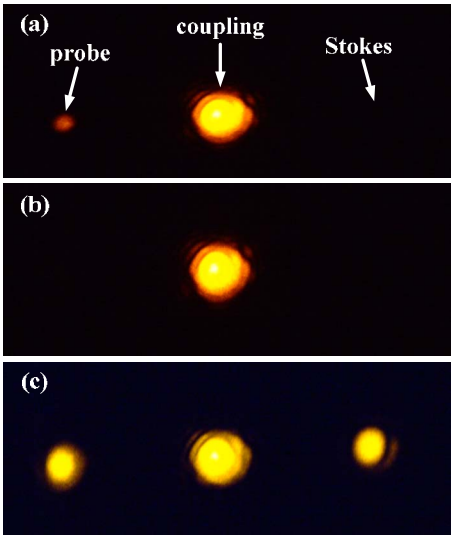

FIG. 2. (Color online) Output beam profiles after the cell (a) when probe is one-photon off-resonant, (b) when probe is one-photon on-resonant, but two-photon off-resonant, and (c) when probe is both one-photon and two-photon on-resonant. All the beams were equally attenuated.

3(a), with the background of the ordinary linear absorption spectrum, three pronounced features were observed when the coupling beam was present. The broad feature at ~1.5 GHz is the incoherent saturated absorption signal when $\nu_p=\nu_c$. We are not interested in this feature but this becomes a convenient marker for knowing that coupling detuning is +1.5 GHz in this case. Two sharp peaks located at ±1.772 GHz from the broad peak are the EIT or PA signals. As can be seen, the peak heights far exceed the line of gain

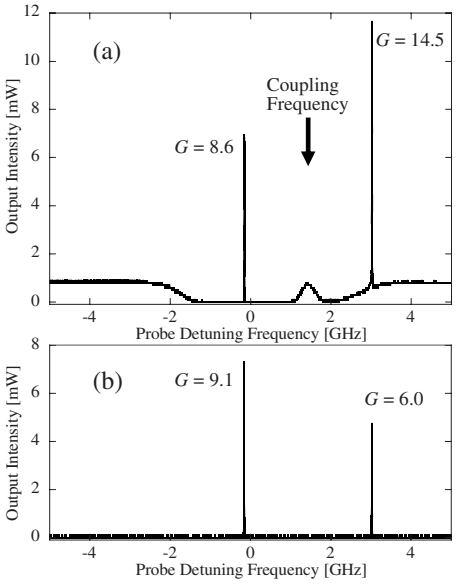

FIG. 3. (a) Typical probe transmission spectrum with the presence of coupling beam. The position of the coupling frequency is indicated by the arrow. (b) Stokes output intensity versus probe detuning frequency. Gains G are also given for the four peaks where G is defined by the output power divided by the input probe power=0.8 mW.

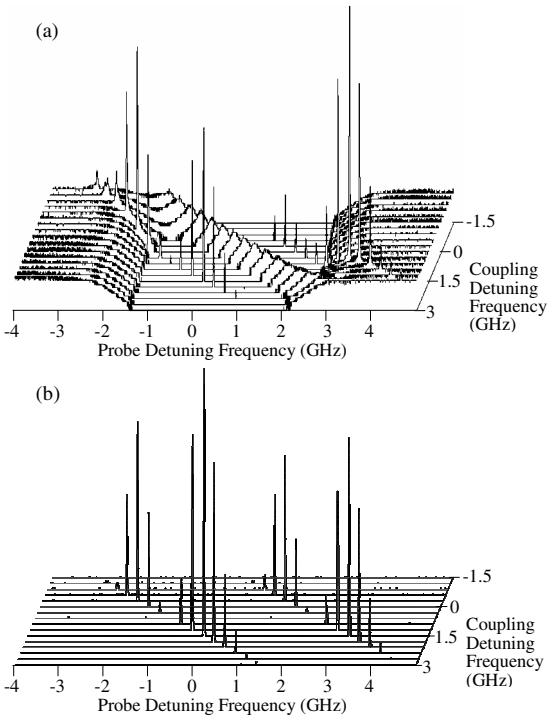

FIG. 4. Three-dimensional plots of (a) probe transmission intensity and (b) output Stokes intensity versus probe detuning and coupling detuning frequencies.

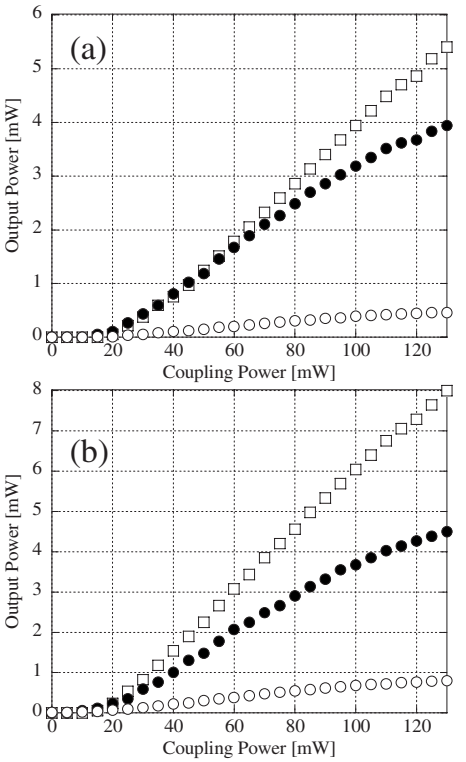

FIG. 5. (a) Probe transmission power versus coupling power and (b) Stokes output power versus coupling power. Open circles, $N=2.6\times10^{11}$ cm^{-3}. Filled circles, $N=3.3\times10^{11}$ cm^{-3}. Open squares, $N=4.4\times10^{11}$ cm^{-3}. Coupling detuning was +1.5 GHz (same as the case of Fig. 3). Probe detuning was red shifted from coupling by 1.772 GHz. Input probe power was 630 μW.

1 (0.8 mW). Gain of 8.6 was obtained even when ν_p was deep in the middle of the absorption line, where $T\approx10^{-5}$ in the absence of the coupling. Therefore, the transmission increased by 6 orders of magnitudes by the presence of the coupling. Even higher gain of up to 14.5 was obtained when ν_p was in the wing of the absorption line similar to the right peak in Fig. 3(a). In a separate experiment with a more sophisticated setup, the highest gains we obtained were 32 in the middle of the absorption line, and 49 in the wing. The Stokes intensity spectrum as a function of ν_p in Fig. 3(b), on the other hand, is much simpler without any background, but the positions of the two sharp peaks precisely correspond to those of Fig. 3(a), and it is clear that probe and Stokes are parametrically coupled and they build up together whenever the two-photon resonance condition is satisfied.

These gain peaks are strongly dependent upon the coupling frequency ν_c, as shown in Figs. 4(a) and 4(b), where the probe transmission spectra and the Stokes intensity spectra are three-dimensionally plotted as functions of ν_p and ν_c. Figures 4(a) and 4(b) clearly show that maximum gain peaks are obtained when coupling detuning is around +1.5 and −0.3 GHz. This is when ν_c is blueshifted or redshifted by ~0.9 GHz from the middle of the absorption line (coupling detuning ~0.6 GHz), and right at the middle, the probe and the Stokes are decoupled and the Stokes output is zero. In this middle point, PA [Fig. 4(b)] is totally nullified but EIT [Fig. 4(a)], or probe transmission, is still observed. Therefore, in this central part of the spectrum, only EIT takes place but PA does not. This problem has been a long time concern to us and quenching of the Stokes generation right at the center of the spectrum has been puzzling in our previous papers [14,15,22]. This problem will be discussed in detail in the theory section.

One should then ask in what situations the system shows an EIT behavior and in which case it is similar to PA. The two main parameters that are experimentally controllable and that determine the situation are the atomic density N (or, equivalently, the peak linear transmissivity T) and the coupling power P_c. We measured the output probe and Stokes intensities as a function of P_c for three different atomic densities N. The results are given in Figs. 5(a) and 5(b) for $N=2.6\times10^{11}$ ($T=1.2\times10^{-3}$), 3.3×10^{11} ($T=2.0\times10^{-4}$), and 4.4×10^{11} cm^{-3} ($T=1.3\times10^{-5}$). When N is low, the probe transmission is low and does not exceed 1 even when P_c is high. High gains are obtained when both N and P_c are high. In this case the probe and Stokes outputs grow linearly with P_c, although eventually the output powers saturate for high enough P_c. Although not shown in the figure, for the lower atomic densities, the Stokes powers are greatly reduced and eventually became zero, meanwhile the probe powers became more and more transparent. These observations are consistent with our previous report [12], where detailed atomic-density dependence of probe and Stokes powers was studied for a rather weak coupling case. The dependences of the probe and Stokes output intensities on N and P_c will be analyzed in detail also in the following section.

III. THEORY

Since our claim is that the SRS process is crucially important in considering the EIT experiment, we treat three modes [coupling (amplitude $\mathcal{E}_c$, frequency ω_c), probe ($\mathcal{E}_p$, ω_p), and Stokes ($\mathcal{E}_s$, ω_s)] interacting with the Λ-type three level system, and study the evolution of probe and Stokes waves under the strong coupling wave [23,24]. The theoretical procedure is the same as our previous paper [12]: (1) Start from the three-mode, three-level Liouville equations, (2) obtain the nonlinear polarizations for probe ($\mathcal{P}_p$) and for Stokes ($\mathcal{P}_s$), and (3) plug these into the Maxwell propagation equations to obtain the coupled propagation equations for probe and Stokes, assuming that the coupling wave is so strong that its depletion during the propagation is neglected. We rewrite the coupled equations in Ref. [12] as

$$\frac{\partial \mathcal{E}_p}{\partial z} = -\frac{\alpha_p}{2}\mathcal{E}_p + c_{pp}|\mathcal{E}_c|^2\mathcal{E}_p + c_{ps}\mathcal{E}_c^2\mathcal{E}_s^*,$$

$$\frac{\partial \mathcal{E}_s}{\partial z} = -\frac{\alpha_s}{2}\mathcal{E}_s + c_{ss}|\mathcal{E}_c|^2\mathcal{E}_s + c_{sp}\mathcal{E}_c^2\mathcal{E}_p^*, \tag{1}$$

where $\alpha_j = kN/(\epsilon_0\hbar)(n_1|p_{31}|^2/\gamma_{j1} + n_2|p_{32}|^2/\gamma_{j2})$ $(j=\{p,s\})$ is the linear absorption coefficient for the probe or the Stokes wave. The four parameters are given as $c_{pp} = A\beta_1/\gamma_{p1}$, $c_{ps} = A\beta_2/\gamma_{p1}$, $c_{ss} = A\beta_2^*/\gamma_{s2}$, and $c_{sp} = A\beta_1^*/\gamma_{s2}$, where $A = kN|p_{31}|^2|p_{32}|^2/(2\epsilon_0\hbar^3)$, $\beta_1 = (n_1/\gamma_{p1} + n_2/\gamma_{c2}^*)/\gamma_0'$, and $\beta_2 = (n_1/\gamma_{c1} + n_2/\gamma_{s2}^*)/\gamma_0'$. $k \sim |\vec{k}_p| \sim |\vec{k}_s|$ is wave vector, N is atomic density, p_{3l} is dipole matrix element for the l-to-3 transition. n_l is the population of the level l and $\gamma_{jl} = \gamma - i(\omega_j - \omega_{3l})$, where $j=\{p,c,s\}$ and $l=\{1,2\}$, and $\gamma_0' = \gamma_s + |\Omega_{c1}|^2/4\gamma_{s2}^* + |\Omega_{c2}|^2/4\gamma_{p1} - i(\omega_0 - \omega_{21})$, where $\Omega_{cl} = (2p_{3l}\mathcal{E}_c)/\hbar$ is the Rabi frequency for the coupling beam. γ and γ_s are the dephasing rates for the optical transitions and the sublevel transition. The interpretation of each term in Eq. (1) is very clear, and the first, the second and the third terms of each equation correspond to linear absorption, EIT, and PA, respectively.

In order to simplify the problem and to obtain analytical solutions for the above equations, we treat the case of two-photon resonance ($\omega_0 = \omega_{21}$), and assume that the two optical transitions have the same dipole moments ($p_{31} = p_{32} \equiv p$ and $\Omega_{c1} = \Omega_{c2} \equiv \Omega_c$). We also assume that the medium is Doppler broadened as $\mathcal{D}(\delta_D) \equiv (2\pi)^{-1/2} g(\delta_D)/\sigma_D$ and $g(\delta_D) \equiv \exp[-\delta_D^2/(2\sigma_D^2)]$, where δ_D is the Doppler shift.

In this case the above equations are simplified as

$$\frac{\partial \mathcal{E}_p}{\partial z} = -\frac{\alpha_0}{2}g(\delta_{c0})(1-\eta_c)\mathcal{E}_p - \frac{\alpha_0\gamma}{2\omega_0}\eta_c\Delta g\mathcal{E}_s',$$

$$\frac{\partial \mathcal{E}_s'}{\partial z} = -\frac{\alpha_0}{2}g(\delta_{c0}+\omega_0)(1-\eta_c)\mathcal{E}_s' - \frac{\alpha_0\gamma}{2\omega_0}\eta_c\Delta g\mathcal{E}_p,$$

where $\delta_{c0} \equiv \omega_{320} - \omega_c$ is the coupling detuning with respect to the transition ω_{320} which is ω_{32} with no Doppler shift (zero atomic velocity). $\mathcal{E}_s' \equiv i\mathcal{E}_s^*$ and $\alpha_0 \equiv \sqrt{\pi/2}kN|p|^2/(\epsilon_0\hbar\sigma_D)$ is the peak linear absorption coefficient, which is roughly proportional to N. $\Delta g \equiv g(\delta_{c0}) - g(\delta_{c0}+\omega_0)$ determines the strength of the Stokes generation and becomes an important factor as we will see below. The saturation parameter η_c is given by

$$\eta_c = \frac{|\Omega_c|^2/4\gamma\gamma_s}{1 + |\Omega_c|^2/4\gamma\gamma_s}, \tag{3}$$

and varies from zero (no coupling case) to 1 (strong coupling regime). Remember that the normalized coupling power $I_c \equiv |\Omega_{c2}|^2/4\gamma\gamma_s$ is given by the ratio of the optical pumping rate $|\Omega_c|^2/4\gamma$ and the sublevel dephasing rate γ_s and this saturation intensity is much smaller than what is needed to saturate the optical transition. The interpretation of Eq. (2) is very straightforward. The last terms of the two equations represent the parametric coupling, and if we neglect them, Eq. (2) is simply reduced to the ordinary EIT process, i.e., the linear absorption of each wave is cancelled by the presence of the factor η_c. In the limit of $\eta_c \to 1$, the medium becomes transparent for both the probe and Stokes waves, but it never amplifies them. If the last terms are included, however, the situation is totally different. In this case the two waves are parametrically coupled and the two waves can be amplified by the proper choice of parameters. In fact, the above equations can be easily analytically solved and the solutions for the initial conditions $\mathcal{E}_p(0) = \mathcal{E}_0$ and $\mathcal{E}_s'(0) = 0$ are given by

$$\mathcal{E}_p(z) = \mathcal{E}_0 e^{-\beta_0 z}\left(\cosh\beta_1 z + \frac{B-A}{2\beta_1}\sinh\beta_1 z\right),$$

$$\mathcal{E}_s'(z) = -\frac{C}{\beta_1}\mathcal{E}_0 e^{-\beta_0 z}\sinh\beta_1 z, \tag{4}$$

where $\beta_0 = (A+B)/2$, $\beta_1 = [(A-B)^2 + 4C^2]^{1/2}/2$, $A = \alpha_0 g(\delta_{c0})(1-\eta_c)/2$, $B = \alpha_0 g(\delta_{c0}+\omega_0)(1-\eta_c)/2$, and $C = \alpha_0\gamma\eta_c\Delta g/(2\omega_0)$.

First we will focus on the efficiency of the Stokes generation, which critically depends on the quantity C. Among all others, C depends on Δg which is the difference of two Gaussians shifted by ω_0 from each other, as shown in Fig. 6(a). Obviously Δg becomes zero when the coupling detuning δ_{c0} is right at the center of the Doppler spectrum. At this point probe and Stokes waves are decoupled and there is no Stokes generation, as we found in the experimental section. Physical interpretation of this quenching effect of the Stokes generation can be made as follows. There are mainly two groups of atoms, type A and B, for contributing the Stokes-wave generation. For a particular group of atoms called type A, as shown in Fig. 6(b), probe is resonant to ω_{31} and coupling resonant to ω_{32}. In this case the atoms are optically pumped to the level 1 by the strong coupling beam and the appropriate Stokes generating process is the one given in Fig. 6(b). (The corresponding double Feynmann diagram is also shown.) On the other hand, for another group of atoms, type B, coupling is resonant to ω_{31} and Stokes resonant to ω_{32}. In this case the atoms are optically pumped to the level 2 and the appropriate Stokes generating process is the one given in Fig. 6(c). Careful theoretical analysis reveals that these two elementary processes have exactly the same magnitudes and the opposite signs. When the coupling is blue (red) detuned from the line center, type B (type A) atoms are

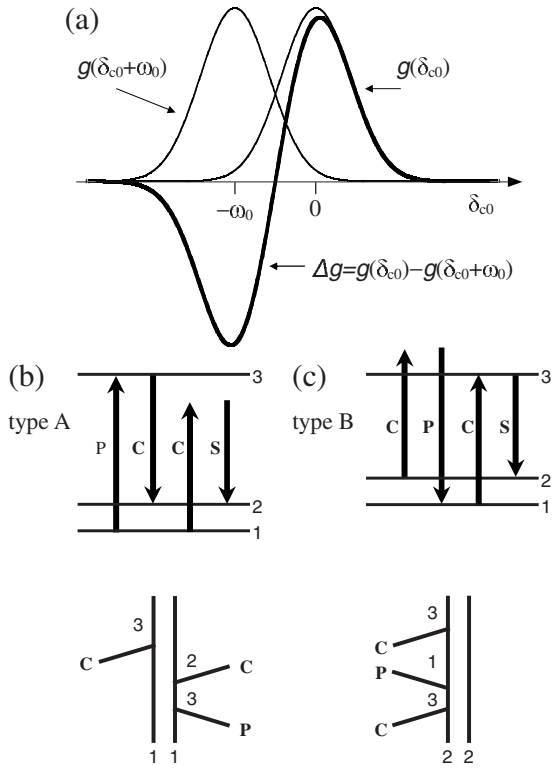

FIG. 6. (a) Two Gaussians $g(\delta_{c0})$ and $g(\delta_{c0}+\omega_0)$ and their difference Δg, when the Doppler width and the hyperfine splitting are comparable. (b) and (c) Elementary processes and corresponding double-Feynman diagrams for type A (b) and type B (c) groups of atoms contributing to the Stokes generation. C: coupling; P: probe; S: Stokes.

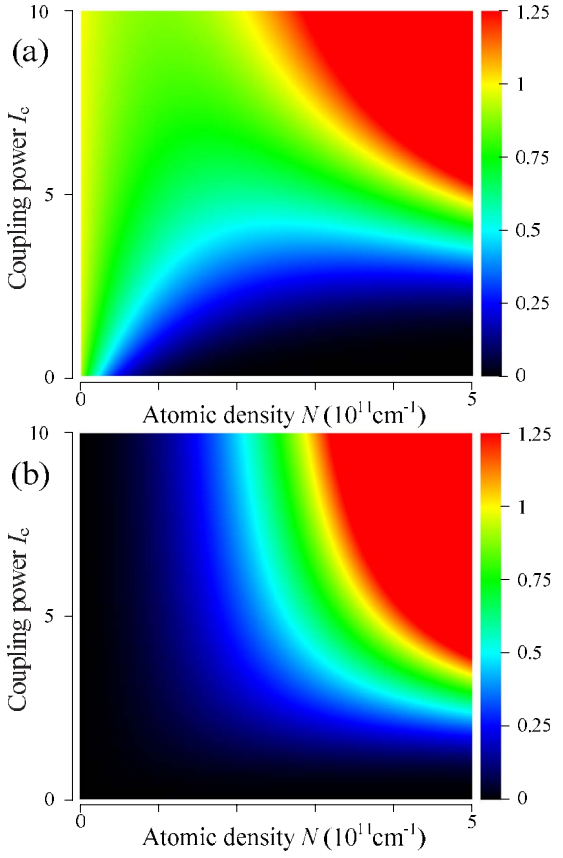

FIG. 7. (Color online) Contour plots of numerical simulation of (a) probe gain and (b) Stokes gain, versus normalized coupling power I_c and atomic density N.

dominant and the Stokes generation takes place. However, right at the center, these two processes cancel and there is no net Stokes generation, and the parametric coupling is nullified. On the other hand, EIT terms [second terms of Eq. (1)] do not have such frequency dependence. Therefore, right at the center [$\delta_{c0}=-\omega_0/2$ in Fig. 6(a)], only EIT (probe transmission) terms remain and PA (Stokes generation) terms disappear, and this fact agrees well with our experimental results. In this way, depending on the coupling frequency the ratio of EIT and PA changes dramatically and it is indeed possible to distinguish EIT and PA contributions.

Lastly and most importantly, we will discuss in which situations the EIT picture is valid and in which case the PA picture is valid. We would like to emphasize that this is simply a matter of parameter setting. The two major parameters (assuming that the coupling detuning δ_{c0} is chosen at the best position) that govern the behavior are (normalized) coupling power I_c and atomic density N. (Note that N is roughly proportional to the peak linear absorption coefficient α_0. They are related such that $\alpha_0=1$ cm^{-1} corresponds to $N=1.75\times10^{11}$ cm^{-3}.) Figure 7 shows the numerically calculated contour plots of the output probe power [Fig. 7(a)] and the output Stokes power [Fig. 7(b)] normalized by the input probe power, as functions of N and I_c and this is our major theoretical results. The parameters are $\delta_{c0}=0$ (this is the situation of Fig. 3), probe detuning is 1.772 GHz higher (Stokes detuning is 1.772 GHz lower) than coupling, and the cell length is 5 cm. The figures may be divided into three different regions. When N is low (in the left half of the figures), Stokes generation can be negligible and the probe transmission T increases as I_c, but T never exceeds 1. This is the region of EIT and the conventional EIT theory works well. In the lower right corners of the figures (high N and low I_c), Stokes is generated as well as probe, but both of them are still less than 1. This may be the region of competition between EIT and SRS as we mentioned earlier in our paper [12]. Finally, in the upper right corners, where both N and I_c are high, both probe and Stokes exceed 1 and parametric amplification is pronounced and the EIT picture breaks down. These theoretical predictions agree very nicely at least quantitatively with the experimental results, Fig. 5, for any atomic densities. Of course detailed behaviors depend on the choice of coupling detuning δ_{c0}, but the above classification is almost universally true.

IV. DISCUSSION AND CONCLUSION

We have confirmed by the experimental and theoretical analyses that, even in ordinary EIT experiments with deeply linear-absorptive situation, the probe wave can be amplified in the presence of strong coupling beam. To obtain high gains, first of all, the coupling frequency must be appropriately detuned to the blue or the red side from the center of

the spectrum for maximum Stokes generation. As parameters of atomic density N and coupling power I_c, the output signal behaviors are divided into three regions. (1) When N is low, the system is safely viewed as EIT, i.e., no probe amplification and no Stokes generation. (2) When N is high but I_c is low, Stokes generation is non-negligible but no amplification is observed. (3) When both N and I_c are high, the probe wave is amplified considerably accompanying generation of Stokes wave with similar intensity. Probe gain up to 32 was observed in an otherwise extremely opaque ($T \sim 10^{-5}$) situation. These findings will lead mainly to two interesting applications. First, one would want to set up a cavity for the Stokes beam and the parametric oscillation should be expected using this extremely high gain medium [20,21]. A novel theory should be established including these concepts for this new type of parametric oscillator, when it is realized. The other direction of this project is to investigate the noise properties of probe and Stokes beams, as extensively studied by McCormick *et al.* [18], leading to the relative intensity squeezing. Although their experiments were performed in transparent regions for the signal and idler waves, our case was performed in a deeply absorptive region. It is quite interesting to investigate noise properties for such a high gain (with coupling) but deeply absorptive (without coupling) medium. We are on the way of these two future directions for the continuation of this research.

[1] K.-J. Boller, A. Imamoğlu, and S. E. Harris, Phys. Rev. Lett. **66**, 2593 (1991).

[2] J. E. Field, K. H. Hahn, and S. E. Harris, Phys. Rev. Lett. **67**, 3062 (1991).

[3] R. Wynands and A. Nagel, Appl. Phys. B: Lasers Opt. **68**, 1 (1999).

[4] M. Merimaa, T. Lindvall, I. Tittonenm, and E. Ikonen, J. Opt. Soc. Am. B **20**, 273 (2003).

[5] M. Fleischhauer and M. D. Lukin, Phys. Rev. Lett. **84**, 5094 (2000).

[6] C. Liu, Z. Dutton, C. H. Behroozi, and L. V. Hau, Nature (London) **409**, 490 (2001).

[7] D. F. Phillips, A. Fleischhauer, A. Mair, R. L. Walsworth, and M. D. Lukin, Phys. Rev. Lett. **86**, 783 (2001).

[8] C. H. van der Wal, M. D. Eisaman, A. André, R. L. Walsworth, D. F. Phillips, A. S. Zibrov, and M. D. Lukin, Science **301**, 196 (2003).

[9] S. E. Harris, Phys. Rev. Lett. **62**, 1033 (1989).

[10] A. Imamoğlu and S. E. Harris, Opt. Lett. **14**, 1344 (1989).

[11] A. S. Zibrov, M. D. Lukin, D. E. Nikonov, L. Hollberg, M. O. Scully, V. L. Velichansky, and H. G. Robinson, Phys. Rev. Lett. **75**, 1499 (1995).

[12] K. Harada, T. Kanbashi, M. Mitsunaga, and K. Motomura, Phys. Rev. A **73**, 013807 (2006).

[13] K. Harada, S. Tanaka, T. Kanbashi, M. Mitsunaga, and K. Motomura, Opt. Lett. **30**, 2004 (2005).

[14] K. Harada, M. Ogata, and M. Mitsunaga, Opt. Lett. **32**, 1111 (2007).

[15] K. Harada, N. Hayashi, K. Mori, and M. Mitsunaga, J. Opt. Soc. Am. **25**, 40 (2008).

[16] V. Wong, R. S. Bennink, A. M. Marino, R. W. Boyd, C. R. Stroud, Jr., and F. A. Narducci, Phys. Rev. A **70**, 053811 (2004).

[17] G. S. Agarwal, T. N. Dey, and D. J. Gauthier, Phys. Rev. A **74**, 043805 (2006).

[18] C. F. McCormick, V. Boyer, E. Arimondo, and P. D. Lett, Opt. Lett. **32**, 178 (2007).

[19] V. Boyer, C. F. McCormick, E. Arimondo, and P. D. Lett, Phys. Rev. Lett. **99**, 143601 (2007).

[20] P. Kumar and J. H. Shapiro, Opt. Lett. **10**, 226 (1985).

[21] M. Poelker and P. Kumar, Opt. Lett. **17**, 399 (1992).

[22] K. Motomura, M. Tsukamoto, A. Wakiyama, K. I. Harada, and M. Mitsunaga, Phys. Rev. A **71**, 043817 (2005).

[23] M. D. Lukin, M. Fleischhauer, A. S. Zibrov, H. G. Robinson, V. L. Velichansky, L. Hollberg, and M. O. Scully, Phys. Rev. Lett. **79**, 2959 (1997).

[24] A. S. Zibrov, M. D. Lukin, and M. O. Scully, Phys. Rev. Lett. **83**, 4049 (1999).